



Journal Name

COMMUNICATION

Formate Adsorption on Pt Nanoparticles during Formic Acid Electro-oxidation: Insights from In Situ Infrared Spectroscopy

Received 00th January 20xx,
Accepted 00th January 20xx

Ian J. McPherson,^a Philip A. Ash,^a Robert M. J. Jacobs^b and Kylie A. Vincent^{*a}

DOI: 10.1039/x0xx00000x

www.rsc.org/

Adsorbed formate is observed on a supported Pt nanoparticle for the first time during formic acid electro-oxidation. Bands assigned to OCO stretching and CH bending reveal some OCO but little CH bond weakening on adsorption compared to the free anion. The formate potential dependence is similar to polycrystalline electrodes while adsorbed CO persists up to +1.2 V, 0.5 V higher than on polycrystalline Pt.

Formic acid oxidation (FAO) is one of the most widely studied reactions in electrocatalysis and is of interest both for direct formic acid fuel cell applications,^{1–4} and more fundamentally in understanding electro-oxidation of small organic molecules to CO₂.^{5,6} The production of formic acid is also likely to be an important step in reverse reactions to capture and utilise CO₂,⁷ and as a possible H₂ storage molecule. Infrared (IR) spectroscopy has been widely used in surface science to examine possible adsorbed intermediates in FAO.⁸ Most work on FAO has focused on the reaction at single- or polycrystalline Pt electrodes, where for a long time a dual pathway mechanism was thought to operate, via direct and indirect pathways involving weakly and strongly adsorbed intermediates, respectively.^{6,9,10} Adsorbed carbon monoxide, CO(ad), was revealed to be the strongly adsorbed intermediate by in situ IR reflection absorption spectroscopy (IRAS).¹¹ The symmetric OCO stretch of adsorbed bridging formate, HCOO(ad), was observed during the reaction using attenuated total reflectance surface enhanced infrared absorption (ATR-SEIRA) experiments on rough Pt films and on this basis HCOO(ad) was assigned as the weakly adsorbed intermediate.^{12–16} Subsequently, the role of HCOO(ad) as an active intermediate has been questioned on the basis that electrocatalytic FAO current is not proportional to the spectroscopically determined coverage of HCOO(ad) either as

a function of potential^{17,18} or of pH.^{19,20} Furthermore a high activation barrier for scission of the C-H bond of HCOO(ad) on Pt (111) has been calculated,^{21–23} although spectroscopic characterisation of the C-H vibrations has not yet been reported during electrocatalytic turnover. Recent opinion, supported by several independent theoretical and experimental studies, now favours the formate anion, HCOO[–] (aq), as the active intermediate.^{19,20,24,25} In this model, HCOO[–] (aq) must approach the surface with its C-H bond down in order to react.²⁵ While some authors suggest existing adsorbates such as HCOO(ad) act to promote this reaction,^{21,26} others consider HCOO(ad) only to block surface sites.^{17,25}

An additional aspect of FAO which must be accounted for in any proposed mechanism is its well-known structure sensitivity, with the rate of both direct and indirect pathways being heavily dependent on the crystallographic orientation of the electrode surface.^{6,10} As well as being of fundamental interest, this structure sensitivity is of great importance for applications, where high surface area electrodes composed of nanoparticles (NPs) are used. NPs can be tailored and modified to present specific surface sites⁴ and therefore in situ characterisation of supported NPs, in addition to single crystal and polycrystalline models, is crucial if the effect of their morphology or composition on the mechanism is to be fully understood. For various reasons (see discussion in Electronic Supplementary Information, ESI section S1), however, CO is the only surface adsorbate that has been studied during FAO on NPs, leaving a gulf between fundamental and applied studies of this important reaction.^{27–29}

Here we present a novel approach to in situ IR spectroscopy of real fuel cell electrocatalysts which allows characterisation of adsorbed intermediates under turnover conditions. We demonstrate it by studying for the first time the behaviour of HCOO(ad) and CO(ad) on a commercial carbon-supported Pt NP catalyst (60% Pt on C, HiSPEC9000 from Johnson Matthey, Pt/C) during sustained FAO. This allows the HCOO(ad)-catalyst interaction to be studied for NPs, and compared with previous reports on model polycrystalline electrodes.

^a Department of Chemistry, University of Oxford, Inorganic Chemistry Laboratory, South Parks Road, Oxford, OX1 3QR

^b Department of Chemistry, University of Oxford, Chemistry Research Laboratory, 12 Mansfield Road, Oxford, OX1 3TA

Electronic Supplementary Information (ESI) available: See DOI: 10.1039/x0xx00000x

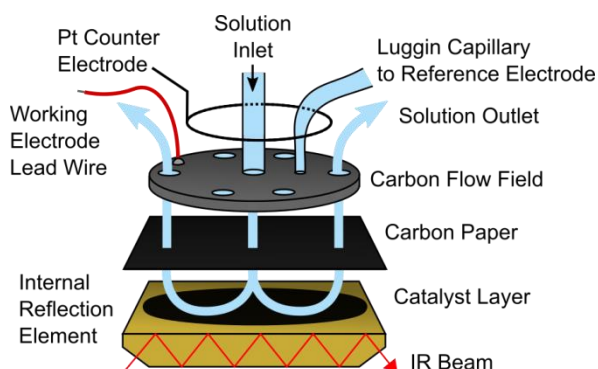


Figure 1. Schematic diagram of the ATR-IR cell developed for this study.

Our approach uses IR spectroscopy in an ATR geometry to sample a thin (ca 2 μm) layer of supported NPs deposited directly onto a silicon internal reflection element (Figure 1 and S1). Electrical connection to the catalyst layer is made via porous carbon paper, eliminating the need for the metal underlayer or solid supporting electrode which are likely to introduce competing reactions or hinder mass transport, respectively (see further discussion in ESI S1). The ATR-IR spectroelectrochemical cell was designed to provide accurate potential control and flow of fuel to the catalyst layer. The effectiveness of the cell is demonstrated in Figure S2, which shows similar electrocatalytic features (although different current densities) in voltammograms of Pt/C catalyst layers on a rotating disc electrode and in the ATR-IR cell, consistent with

previous reports of FAO on polycrystalline Pt,¹⁸ or a similar Pt/C catalyst.³⁰

Figure 2A shows IR spectra of the Pt/C layer obtained in situ during a slow cyclic voltammogram (scan rate 1 mV s^{-1}) in HCOOH (25 mM). The spectra show potential-dependent peaks at 2343, 2035-2046, 1811-1827, 1600-1450, 1384, 1315 and 1250 cm^{-1} . Of these peaks, four can be assigned with reference to previous ATR-SEIRA data: the asymmetric stretch of dissolved CO_2 , $\nu(\text{CO}_2) = 2343 \text{ cm}^{-1}$; the C-O stretch of linear adsorbed CO, $\nu(\text{CO}_\text{L}) = 2035\text{-}2046 \text{ cm}^{-1}$; the C-O stretch of bridging adsorbed CO, $\nu(\text{CO}_\text{B}) = 1811\text{-}1827 \text{ cm}^{-1}$; and the OCO symmetric stretch of adsorbed bridging HCOO(ad) , $\nu_\text{s}(\text{OCO}) = 1315 \text{ cm}^{-1}$.^{12,13,31} An analogous experiment was performed on a film comprising only the carbon support (without Pt) in HClO_4 and is shown in Figure S3. This suggests that the peaks around 1250 and 1570 cm^{-1} can be assigned to functional groups on the surface of the carbon support,^{32,33} as shown in Figure 2B. These assignments are all consistent with the observed shifts in peak position when the experiment is repeated in ^{13}C -labelled HCOOH (Figure S4). The $\nu_\text{s}(\text{OCO})$ shifts to 1294 cm^{-1} as shown in Figure 2C, confirming that this peak originates from HCOOH. Assignment of the remaining peak at 1384 cm^{-1} can be made by comparison with the solution spectrum of NaOOCH (Figure 2E) in which a peak at 1384 cm^{-1} is assigned to the in-plane C-H bend, $\delta(\text{CH})$, and is insensitive to ^{13}C substitution.³⁴

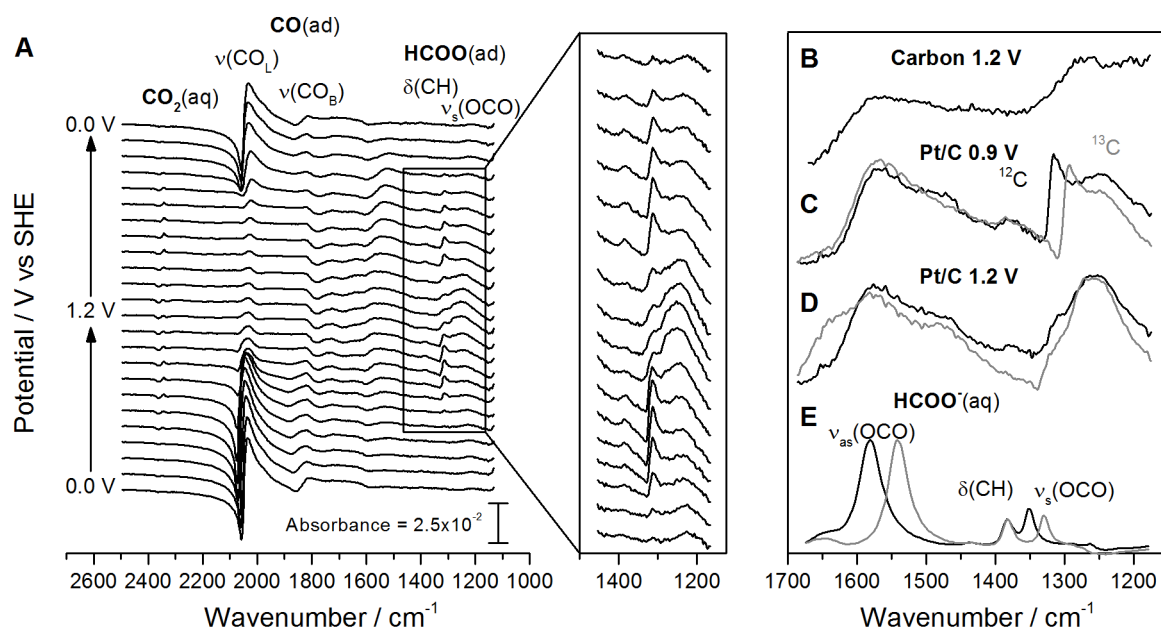


Figure 2. Infrared spectra of A) Pt/C catalyst layer during cyclic voltammetry in 25 mM HCOOH + 0.5 M HClO_4 . Scan rate = 1 mV s^{-1} . Interval between spectra = 100 mV. Background = 0 V before addition of HCOOH. B) Carbon black support in HClO_4 at 1.2 V. C) Pt/C at 0.9 V recorded during cyclic voltammetry in unlabeled (black) and ^{13}C -labelled (gray) HCOOH. Background = 0.2 V in the cycle. D) As C except at 1.2 V. E) Natural abundance (black) and ^{13}C -labelled (gray) NaOOCH solution (0.1 M). Background = water. Spectra in B-E normalized to their maximum intensities.

The 1384 cm^{-1} peak in the Pt/C spectra is also insensitive to ^{13}C substitution and is therefore tentatively assigned to the $\delta(\text{CH})$ mode of HCOO(ad) .

Figure 3A shows the cyclic voltammogram recorded during collection of the spectra in Figure 2A, along with the potential dependence of the $\delta(\text{CH})$, $\nu_\text{s}(\text{OCO})$ and $\nu(\text{CO}_\text{L})$ peaks (Figure 3B, C and D respectively).

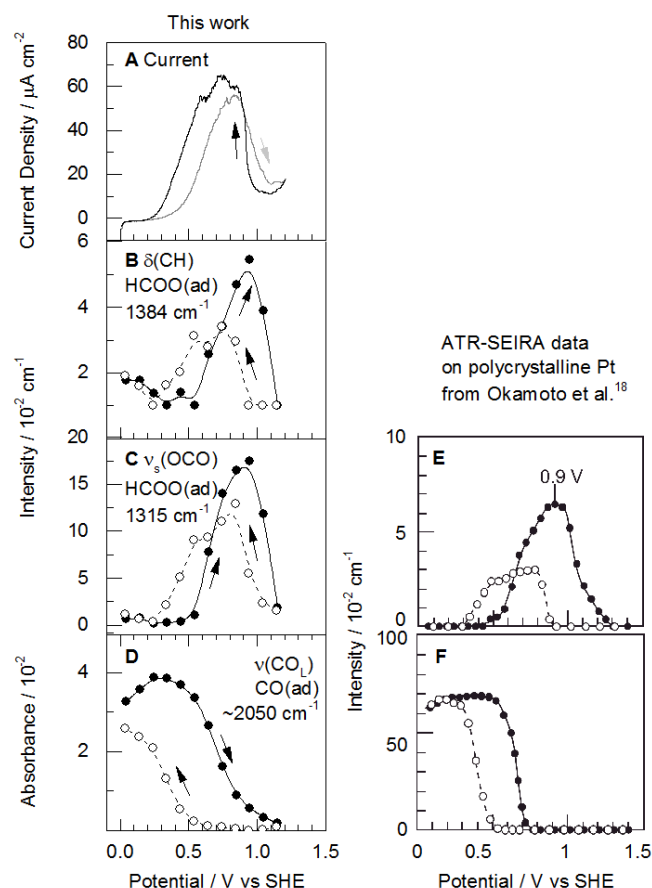


Figure 3: The observed current density (A), integrated peak intensities of the $\delta(\text{CH})$ (B) and $\nu_s(\text{OCO})$ (C) modes of HCOO(ad) and the absorbance of the $\nu(\text{CO}_L)$ peak (D) of CO(ad) as a function of potential during the voltammogram. Lines are included as a guide only. Arrows indicate the direction of the scan. These data were derived from the spectroelectrochemical experiment presented in Figure 2A. Comparison of the potential dependencies of CO(ad) and HCOO(ad) during cyclic voltammetry experiments at 1 mV s^{-1} on Pt/C (Panels C and D) and a Pt thin layer studied using ATR-SEIRA by Okamoto et al. (Panels E and F) is made.¹⁸ Panels E and F reprinted from *Electrochimica Acta*, Volume 116, Okamoto, H., Numata, Y., Gojuki, T. and Mukouyama, Y., Different behavior of adsorbed bridge-bonded formate from that of current in the oxidation of formic acid on platinum, Pages 263-270, Copyright © 2014, with permission from Elsevier.

While the integrated area is shown for the HCOO(ad) peaks, the bipolar shape of the $\nu(\text{CO}_L)$ peak (often observed for CO on NP films)^{35–38} complicates peak integration. The $\nu(\text{CO}_L)$ peak intensity is therefore approximated by the positive maximum absorbance in the range $2035\text{--}2046 \text{ cm}^{-1}$. Further discussion of the data handling is provided in section S4 of the Supporting Information (see Figures S5 and S6). At the start of the sweep the current is negligible and the spectra are dominated by $\nu(\text{CO}_L)$. At potentials above 0.4 V the $\nu(\text{CO}_L)$ peak absorbance decreases monotonically, and the oxidation current begins to increase. Conversely the $\nu_s(\text{OCO})$ and $\delta(\text{CH})$ peaks only appear above 0.5 V and share the same potential dependence during both the positive and negative sweeps, providing further evidence for assignment of these peaks to the same species, HCOO(ad) . This represents the first observation of HCOO(ad) during FAO on supported NPs and only the second report of

the $\delta(\text{CH})$ mode on any metal surface, the first coming from HCOOH adsorption in UHV on the corrugated Pt(110)(1\times2) surface.³⁹ The absence of the $\delta(\text{CH})$ mode from spectra has been explained by the surface selection rule (SSR)^{12,40,41} which states that vibrations with dipole moments parallel to metal surfaces are not observed.^{42–44} HCOO(ad) is a bridging species bound to 2 Pt atoms through its 2 O atoms, almost perpendicular to the surface.^{12,40,41} In this position the dipole moment of the C-H wagging mode is parallel to the surface and therefore usually IR inactive due to the SSR. When the SSR on metal particles was first discussed quantitatively by Greenler, weakening of the rule was predicted for particle sizes $< 2 \text{ nm}$, based on the curvature of their surface.⁴³ The quoted size of the particles used in this work is 4.75 nm, 1–2 orders of magnitude smaller than the NP curvature of the metal films used in ATR-SEIRA,⁴⁵ and of the same order as the predicted threshold for weakening of the SSR. This small particle size would therefore account for observation of the $\delta(\text{CH})$ mode in this work.

The $\delta(\text{CH})$ mode is significant as it reports on the C-H bond of HCOO(ad) . This bond is important as its scission would be the final step, were CO_2 to be produced from HCOO(ad) , and as a result the barrier to this process helps determine the extent to which HCOO(ad) decomposition contributes to FAO. The present finding, that the position of the $\delta(\text{CH})$ peak remains unperturbed from its value in $\text{HCOO}^-(\text{aq})$, indicates that there is no significant activation of the C-H bond when HCOO adsorbs on pure Pt, lending weight to recent proposals that HCOO(ad) is a spectator species during formic acid oxidation on Pt.^{17,24,25} This finding is also in agreement with DFT calculations which predict that the majority of electron density accepted by HCOO on adsorption on Pt is localized in the conjugated π system of OCO^- ,²¹ leaving a high activation energy for CH bond scission.^{21–23}

The ATR-IR experiments described here provide the first spectroscopic evidence that a significant surface coverage of HCOO(ad) is present during electrocatalytic formic acid oxidation on Pt nanoparticles, and make it possible to compare differences in reactivity between supported metal NPs and polycrystalline electrodes. The wavenumber position of the $\nu_s(\text{OCO})$ mode observed on the NPs is around 10 cm^{-1} lower than that reported in ATR-SEIRA measurements on thin-layer Pt electrodes,¹² suggesting a stronger interaction between HCOO(ad) and the NPs. Figure 3E and F show, for comparison, the potential dependence of the $\nu_s(\text{OCO})$ and $\nu(\text{CO}_L)$ peaks recorded from SEIRA experiments on polycrystalline Pt by Okamoto et al. at the same scan rate and 100 mM HCOOH in 0.5 M H_2SO_4 .¹⁸ The potential dependence of HCOO(ad) on the NPs is very similar to that in the SEIRA Pt thin-layer measurements (Figure 3C,E), although the NPs exhibit a more positive onset potential for HCOO adsorption during the reverse potential sweep. This could reflect the stronger interaction between HCOO(ad) and the NPs, although it may simply result from a thicker oxide layer arising from the higher anodic potential limit used in the ATR-SEIRA experiment. On the other hand, CO persists on the NP surface to higher potentials on the forward sweep (Figure 3D,F) compared with

the thin-layer electrode, consistent with the much higher onset potential reported for CO oxidation on small NPs compared with bulk Pt.^{46–48,27} This suggests that differences in FAO between NPs and bulk Pt are likely to arise from changes to the indirect pathway rather than from HCOO(ad).

The ATR-IR spectroelectrochemical approach we describe here should enable FAO to be investigated on more complex NP catalysts with respect to the roles of both CO(ad) and HCOO(ad) in catalysis and poisoning. More generally this technique is applicable to the study of the effects of metal NP composition and morphology on the electrocatalytic activation of many other small molecules.

Notes and references

- We are grateful to Jonathan Quinson for SEM. We acknowledge Ean Ong and Juan Liu for preliminary work and the staff of the Mechanical Workshop (Department of Chemistry) for assistance with cell design and fabrication. This work was supported financially by the European Research Council (ERC, EnergyBioCatalysis-ERC-2010-StG-258600, IJM, PAA and KAV).
- C. Rice, S. Ha, R. I. Masel, P. Waszczuk, A. Wieckowski and T. Barnard, *J. Power Sources*, 2002, **111**, 83–89.
 - X. Yu and P. G. Pickup, *J. Power Sources*, 2008, **182**, 124–132.
 - N. V. Rees and R. G. Compton, *J. Solid State Electrochem.*, 2011, **15**, 2095–2100.
 - C. A. Rice, A. Bauskar and P. G. Pickup, in *Electrocatalysis in Fuel Cells*, ed. M. Shao, Springer London, 2013, pp. 69–87.
 - T. D. Jarvi and E. M. Stuve, in *Electrocatalysis*, Wiley-VCH, New York; Chichester, 1998, vol. Lipkowski, Jacek; Ross Philip N. (eds.), pp. 75–153.
 - J. M. Feliu and E. Herrero, in *Handbook of Fuel Cells*, John Wiley & Sons, Ltd, 2010, vol. 2.
 - J. Qiao, Y. Liu, F. Hong and J. Zhang, *Chem. Soc. Rev.*, 2013, **43**, 631–675.
 - N. R. Avery, *Appl. Surf. Sci.*, 1983, **14**, 149–156.
 - A. Capon and R. Parsons, *J. Electroanal. Chem. Interfacial Electrochem.*, 1973, **45**, 205–231.
 - J. Clavilier, R. Parsons, R. Durand, C. Lamy and J. M. Leger, *J. Electroanal. Chem. Interfacial Electrochem.*, 1981, **124**, 321–326.
 - B. Beden, A. Bewick and C. Lamy, *J. Electroanal. Chem. Interfacial Electrochem.*, 1983, **150**, 505–511.
 - A. Miki, S. Ye and M. Osawa, *Chem. Commun.*, 2002, 1500–1501.
 - G. Samjeské, A. Miki, S. Ye and M. Osawa, *J. Phys. Chem. B*, 2006, **110**, 16559–16566.
 - M. Osawa, K. Komatsu, G. Samjeské, T. Uchida, T. Ikeshoji, A. Cuesta and C. Gutiérrez, *Angew. Chem. Int. Ed.*, 2011, **50**, 1159–1163.
 - A. Cuesta, G. Cabello, M. Osawa and C. Gutiérrez, *ACS Catal.*, 2012, **2**, 728–738.
 - A. Cuesta, G. Cabello, C. Gutiérrez and M. Osawa, *Phys. Chem. Chem. Phys.*, 2011, **13**, 20091.
 - Y.-X. Chen, M. Heinen, Z. Jusys and R. J. Behm, *Langmuir*, 2006, **22**, 10399–10408.
 - H. Okamoto, Y. Numata, T. Gojuki and Y. Mukouyama, *Electrochimica Acta*, 2014, **116**, 263–270.
 - J. Joo, T. Uchida, A. Cuesta, M. T. M. Koper and M. Osawa, *J. Am. Chem. Soc.*, 2013, **135**, 9991–9994.
 - S. Brimaud, J. Solla-Gullón, I. Weber, J. M. Feliu and R. J. Behm, *ChemElectroChem*, 2014, **1**, 1075–1083.
 - H.-F. Wang and Z.-P. Liu, *J. Phys. Chem. C*, 2009, **113**, 17502–17508.
 - M. Neurock, M. Janik and A. Wieckowski, *Faraday Discuss.*, 2009, **140**, 363.
 - W. Gao, J. A. Keith, J. Anton and T. Jacob, *J. Am. Chem. Soc.*, 2010, **132**, 18377–18385.
 - J. Joo, T. Uchida, A. Cuesta, M. T. M. Koper and M. Osawa, *Electrochimica Acta*, 2014, **129**, 127–136.
 - K. A. Schwarz, R. Sundararaman, T. P. Moffat and T. C. Allison, *Phys Chem Chem Phys*, 2015, **17**, 20805–20813.
 - J. V. Perales-Rondón, E. Herrero and J. M. Feliu, *Electrochimica Acta*, 2014, **140**, 511–517.
 - K. Kunitatsu, T. Sato, H. Uchida and M. Watanabe, *Langmuir*, 2008, **24**, 3590–3601.
 - A. M. Hofstead-Duffy, D.-J. Chen, S.-G. Sun and Y. J. Tong, *J. Mater. Chem.*, 2012, **22**, 5205.
 - A. M. Hofstead-Duffy, D.-J. Chen and Y. J. Tong, *Electrochimica Acta*, 2012, **82**, 543–549.
 - S. Park, Y. Xie and M. J. Weaver, *Langmuir*, 2002, **18**, 5792–5798.
 - D. S. Corrigan and M. J. Weaver, *J. Electroanal. Chem.*, 1988, **241**, 143–162.
 - M. S. Akhter, J. R. Keifer, A. R. Chughtai and D. M. Smith, *Carbon*, 1985, **23**, 589–591.
 - F. Rositani, P. L. Antonucci, M. Minutoli, N. Giordano and A. Villari, *Carbon*, 1987, **25**, 325–332.
 - K. G. Kidd and H. H. Mantsch, *J. Mol. Spectrosc.*, 1981, **85**, 375–389.
 - W. Chen, S.-G. Sun, Z.-Y. Zhou and S.-P. Chen, *J. Phys. Chem. B*, 2003, **107**, 9808–9812.
 - Z.-F. Su, S.-G. Sun, C.-X. Wu and Z.-P. Cai, *J. Chem. Phys.*, 2008, **129**, 44707.
 - C. Pecharrromán, A. Cuesta and C. Gutiérrez, *J. Electroanal. Chem.*, 2002, **529**, 145–154.
 - C. Pecharrromán, A. Cuesta and C. Gutiérrez, *J. Electroanal. Chem.*, 2004, **563**, 91–109.
 - T. Ohtani, J. Kubota, A. Wada, J. N. Kondo, K. Domen and C. Hirose, *Surf. Sci.*, 1996, **368**, 270–274.
 - N. R. Avery, *Appl. Surf. Sci.*, 1982, **11–12**, 774–783.
 - P. Hofmann, S. R. Bare, N. V. Richardson and D. A. King, *Surf. Sci.*, 1983, **133**, L459–L464.
 - R. G. Greenler, *J. Chem. Phys.*, 1966, **44**, 310.
 - R. G. Greenler, D. R. Snider, D. Witt and R. S. Sorbello, *Surf. Sci.*, 1982, **118**, 415–428.
 - H. A. Pearce and N. Sheppard, *Surf. Sci.*, 1976, **59**, 205–217.
 - H. Miyake, S. Ye and M. Osawa, *Electrochem. Commun.*, 2002, **4**, 973–977.
 - K. A. Friedrich, F. Henglein, U. Stimming and W. Unkauf, *Electrochimica Acta*, 2000, **45**, 3283–3293.
 - F. Maillard, M. Eikerling, O. V. Cherstiouk, S. Schreier, E. Savinova and U. Stimming, *Faraday Discuss.*, 2004, **125**, 357.
 - F. Maillard, E. R. Savinova and U. Stimming, *J. Electroanal. Chem.*, 2007, **599**, 221–232.